CORROSION ENGINEERING, SCIENCE AND TECHNOLOGY
2023, VOL. 58, NO. 6, 561–566
https://doi.org/10.1080/1478422X.2023.2238388

I·M3 Institute of Materials, Minerals & Mining

Taylor & Francis
Taylor & Francis Group

RESEARCH ARTICLE

Sulfidation kinetics of titanium and Ti-6Al-4V with elemental sulfur

Subbarao Raikar, Steven DiGregorio and Owen J. Hildreth

Department of Mechanical Engineering, Colorado School of Mines, Golden, CO, USA

ABSTRACT

The sulfidation kinetics of titanium and Ti-6Al-4V (Ti64) using elemental sulfur were studied by measuring the amount of metal consumed instead of the change in mass or scale thickness. This metal consumption approach combines the parabolic oxidation law, Arrhenius equation, and Pilling-Bedworth ratio to determine the apparent activation energy and the pre-exponential factor of consumption of Ti64 during sulfidation. The estimations of apparent activation energy and pre-exponential factor were 110.4 kJ·mol^{-1} and 1.3×10^{-9} m^{2}s^{-1} for the titanium-sulfur, and 116.2 kJ·mol^{-1} and 1.2×10^{-9} m^{2}s^{-1} for the Ti64-sulfur system. Finally, a material removal predictor was developed to predict the amount of Ti64 consumed for a given sulfidation temperature and time.

ARTICLE HISTORY
Received 28 January 2023
Accepted 15 July 2023

KEYWORDS
Sulfidation; kinetics; Ti-6Al-4V; titanium; post-processing; additive manufacturing

Introduction

Understanding the corrosion kinetics of sulfur-metal systems is of great interest for preventing or mitigating the detrimental effects of corrosion in industries such as oil and gas power plants [1,2]. Corrosion kinetics are also of interest to the Additive Manufacturing (AM) industry, which uses controlled corrosion to remove metal support structures and improve the surface finish and fatigue performance of printed parts [3–6]. The Hildreth Group recently developed techniques that use sulfidizing corrosive environments for post-processing additively manufactured Ti-6Al-4V (Ti64) parts [5]. In these techniques, a 3D-printed metal part is heat-treated in a sulfur environment to form sulfide scales with the top 50–100 µm of the part's surface. A solution of sulfuric acid and sodium molybdate selectively dissolves these sulfide scales while protecting the base alloy. Since these corrosion-based techniques consume material from the surface of the alloys, parts need oversizing to account for the material removed for functional accuracy. One can determine the amount of material consumed for a given process temperature and time by studying the kinetics of the solid–gas interaction, i.e. Ti64-sulfur interaction. Several studies exist for the sulfidation of Ti64 and other alloys in the presence of gaseous H_2S or SO_2 [7–11]; however, to the authors best knowledge, no literature exists on the sulfidation of Ti64 with elemental sulfur. This work aimed to fill that knowledge gap. In addition, a material removal prediction model was developed using the kinetic parameters. The material removal predictor can help post-processing engineers to create recipes to remove a fixed amount of material from the surface of an AM part.

Gas–solid kinetics can be determined from the amount of metal consumed or the amount of scale formed by measuring their respective change in mass or thickness [12]. A popular and convenient method to study the gas–solid kinetics of scale growth during oxidation and sulfidation is thermogravimetric analysis (TGA) [13]. In the TGA approach, a metal sample is suspended from a spring in the middle of a vertical tube furnace, which is attached to a balance to measure the continuous change in sample mass during the reaction. After the sample has reached the desired temperature, a reactive gas, such as oxygen, sulfur, iodine, or a mixture of gases, flows from the bottom of the tube furnace. The gas reacts with the metal surface to form a scale, which continues to grow as the species diffuses through the scale to propagate the reaction. TGA relies on measuring the mass change of the metal sample *in situ* to estimate the kinetic parameters. This *in situ*, TGA-based approach for measuring scale formation kinetics can be improved by accounting for the change in the metallic core during the reaction [14,15].

While TGA is an excellent tool for accurately measuring scale formation kinetics, the equipment can be extremely expensive, especially if the feedstock for the corrosive gas is a solid or a liquid. This cost can be avoided by measuring the scale thickness *ex situ* while varying reaction temperatures and reaction times [16–18]. However, measuring the scale thickness is challenging and inaccurate in systems with fragile scales, such as Ti64-sulfur. Therefore, this work used the amount of metal consumed to determine the gas–solid kinetics of a Ti64-sulfur system. In this work, the material consumption approach is described and the formulae to determine the apparent activation energy and pre-exponential factor were derived. The material consumption approach was validated with the titanium-sulfur system against Ohta et al. [19], and Dutrizac [20], and then extended to the Ti64-sulfur system to develop the material removal predictor to estimate the amount of Ti64 removed from the surface for a given sulfidation temperature and time.

Materials and methods

Sample preparation

A 254 µm thick Ti64 sheet (TMS Titanium) and a 200 µm thick titanium sheet (Futt) were cut into 14 mm × 10 mm pieces using a sheet metal shearing machine. The Ti64 and

CONTACT Owen J. Hildreth ohildreth@mines.edu Department of Mechanical Engineering, Colorado School of Mines, 1500 Illinois St., Golden, CO 80401, USA

Supplemental data for this article can be accessed online at https://doi.org/10.1080/1478422X.2023.2238388.

titanium sheet pieces were cleaned in an ultrasonic bath with acetone, methanol, and isopropyl alcohol for 5 min. Next, the sheet pieces were blow-dried with compressed N_2 gas (General Air). All the cleaned sheet pieces were placed individually in a fused quartz tube (13X16, Technical Glass) of length 300 mm with 25 mg of sulfur flakes (≥99.99% trace metals basis, Sigma Aldrich). The fused quartz tube was then purged with Ar (99.999%, General Air), evacuated three times, and sealed with a hydrogen–oxygen flame in the evacuated state. The length of the fused quartz was 300 mm to prevent an explosion due to excessive internal pressure in the tube. The samples encapsulated in the fused quartz tubes were placed in a box furnace (Carbolite 201) after the temperature was equilibrated for sulfidation. Supplementary Information Figure S1 shows a representative image of the encapsulated samples. After four hours of sulfidation, the encapsulated samples in the furnace were quenched in water to arrest the sulfidation reaction. The samples were sulfidized in steps of 100°C from 650°C to 950°C for 4 h to fit the linearised metal consumption model. Finally, the sulfidized sheet samples were removed from the fused quartz tube for analysis. The sulfide scales formed on the sheet samples were fragile and easily broke away when the samples were removed from the tube.

Characterisation

Sheet samples were mounted along the longer edge in a mixture of mounting copper powder (Allied High-tech) and cold-curing epoxy (EpoFix, Struers) within 1.25-inch diameter mold cups. After mounting, the samples were ground with sequentially finer media starting with silicon carbide paper ranging from 180 grit to 600 grit, then polished with 9 µm diamond suspension and 0.05 µm colloidal silica. The samples were thoroughly rinsed with deionised water after each grinding step, and in addition dried with compressed N_2 gas after the last grinding step and between each polishing step. The polished cross-section samples were then imaged at 10 locations with an inverted optical microscope (Zeiss Axio Vert. A1) to measure the thickness of the Ti64 and titanium sheets after sulfidation. The cross-sectioned samples were also imaged in a TESCAN MIRA3 Scanning Electron Microscope (SEM) to characterise the sulfide scale if present. X-ray Diffraction (XRD) data of the scale was collected with Bruker D2 Phaser with a cobalt source. The scale was held in place on a silicon holder using polytetrafluoroethylene (PTFE) grease. The XRD diffractogram was analysed with Bruker's DIFFRAC. EVA and PDF-4/Axiom database from International Centre for Diffraction Data (ICDD) [21].

Theory

System and material consumption approach description

In the Ti64-sulfur system, sulfur adsorbs on the Ti64 surface and reacts with it to form a thin layer of sulfides. The subsequent sulfide layers primarily form at the sulfides-gas interface because of the outward diffusion of the cations from the Ti64-sulfides interface, which is significantly faster than the diffusion of sulfur through the scale [22]. Figure 1 shows a schematic diagram of the growth of the sulfide scale in the Ti64-sulfur system. The cations are mainly titanium since Ti64 alloy primarily consists of titanium. The XRD diffractogram, in Figure 2, indicates that the primary phase identified in the scale is TiS_2, corroborating the significantly greater presence of titanium ions compared to aluminium and vanadium ions. In addition, elemental maps of the cross-section of a sulfidized Ti64 sheet are also included in the Supplementary Information Figure S2 as a visual confirmation.

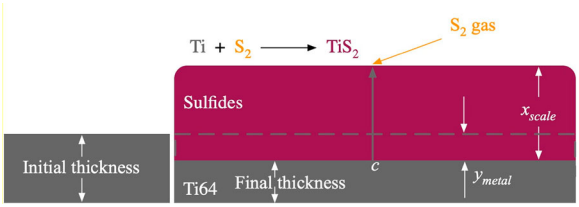

Figure 1. Schematic diagram of the sulfide scale growth in Ti64-sulfur system.

The sulfidation kinetics of the Ti64-sulfur system can be studied using the parabolic oxidation law [17], which captures the growth of the sulfide scale by relating the sulfide scale thickness to sulfidation time. However, this model is difficult to use for fragile scales, and the broken scale shown in Figure 3 shows this problem, with the scale deforming at multiple locations. This work used the amount of substrate material consumed to accurately measuring the scale thickness.

Metal consumption model derivation

The material consumption approach measured the metal consumed thickness (difference between initial and final thicknesses) instead of the more inaccurate measurement of sulfide scale thickness. The material consumption approach was derived from the parabolic oxidation law, the Pilling-Bedworth ratio, and the Arrhenius law. This approach works only if the material consumption is uniform and if no intergranular ingress of the corrosion species occurs. Figure 4 shows a schematic diagram and optical images of the cross-section of the metal sheet before and after sulfidation. Figure 4 also illustrates the different thicknesses measured in the different approaches, i.e. scale thickness when using the parabolic oxidation law and metal consumed thickness when using the metal consumption model.

The parabolic oxidation law Equation 1 [17] is a relationship between the scale thickness and the reaction time for a given reaction temperature:

$$\frac{x_{scale}^2}{2D} + \frac{x_{scale}}{k'} = \frac{ct}{G} \tag{1}$$

where x_{scale} = thickness of the scale $[m]$, D = diffusion coefficient $[m^2 \cdot s^{-1}]$, k' = reaction rate $[m \cdot s^{-1}]$, c = concentration of the cations at the metal-scale interface $[mol \cdot m^{-3}]$, t = sulfidation time $[s]$, and G = growth thickness constant $[mol \cdot m^{-3}]$.

In the parabolic oxidation law, the first term represents the scale growth under the diffusion-controlled regime and the second term represents the scale growth under the reaction-controlled regime. Strafford established that scale growth during sulfidation is primarily diffusion-controlled [22]. Therefore, only the first term of the parabolic oxidation law was considered for simplicity. The parabolic

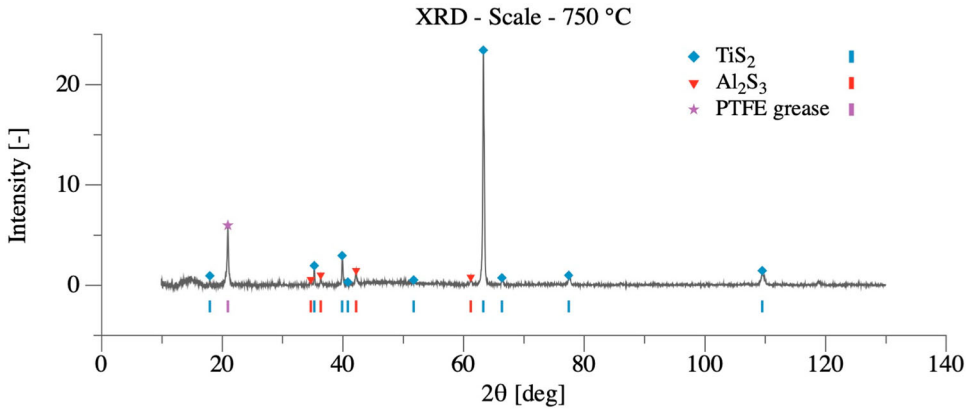

Figure 2. XRD diffractogram of the sulfide scale showing TiS_2 as the primary phase.

law reduces to:

$$\frac{x_{scale}^2}{2D} = \frac{ct}{G} \tag{2}$$

Equation (2) predicts the thickness of the scale for a given sulfidation time at one sulfidation temperature, since the diffusion coefficient is a temperature-dependent parameter. The diffusion coefficient can be determined empirically by fitting the reduced parabolic oxidation law. Since the scale thickness cannot be measured accurately due to its fragility, the reduced parabolic oxidation law was modified with the Pilling-Bedworth ratio (PB), which relates the volume of the scale to the volume of the metal in the scale, and is used to predict the passivation behaviour of scales [23]:

$$PB = \frac{V_{scale}}{V_{metal}} = \frac{M_{sulfide} \cdot \rho_{metal}}{n \cdot M_{metal} \cdot \rho_{sulfide}} \tag{3}$$

where V_{scale} = volume of sulfide $[m^3]$, V_{metal} = volume of the metal in the sulfide $[m^3]$, M_{scale} = molecular mass of sulfide $[g{\cdot}mol^{-1}]$, ρ_{metal} = density of metal $[kg{\cdot}m^{-3}]$, n = number of atoms of the metal per a molecule of sulfide, M_{metal} = molecular mass of the metal in the sulfide $[g{\cdot}mol^{-1}]$, and ρ_{scale} = density of the sulfide $[kg{\cdot}m^{-3}]$. The metal and scale volumes can also be determined, as shown Equation 4. This relationship can be simplified since the surface through which ion diffusion takes place is the same as the surface of the metal, i.e. the area of the sulfide is equal to the area of the metal consumed [14].

$$PB = \frac{V_{scale}}{V_{metal}} = \frac{A_{scale} \cdot x_{scale}}{A_{metal} \cdot y_{metal}} = \frac{x_{scale}}{y_{metal}} \tag{4}$$

where A_{scale} = area of sulfide $[m^2]$, A_{metal} = area of the metal in the sulfide $[m^2]$, x_{scale} = thickness of the scale $[m]$, and y_{metal} = thickness of metal consumed $[m]$. Combining both Equations 3 and 4, we establish a relationship between the scale thickness and the metal consumed thickness.

$$x_{scale} = \left(\frac{M_{sulfide} \cdot \rho_{metal}}{n \cdot M_{metal} \cdot \rho_{sulfide}} \right) \cdot y_{metal} \tag{5}$$

Using Equation 5, the scale thickness in the reduced parabolic oxidation law was substituted with the metal consumed thickness. The reduced parabolic oxidation law in terms of metal consumed thickness is:

$$\left(\frac{M_{sulfide} \cdot \rho_{metal}}{n \cdot M_{metal} \cdot \rho_{sulfide}} \right)^2 \frac{y_{metal}^2}{2D} = \frac{ct}{G} \tag{6}$$

All the material and transport properties were combined into one property called the metal consumption coefficient (C_{Ti}). The consumption coefficient is analogous to the

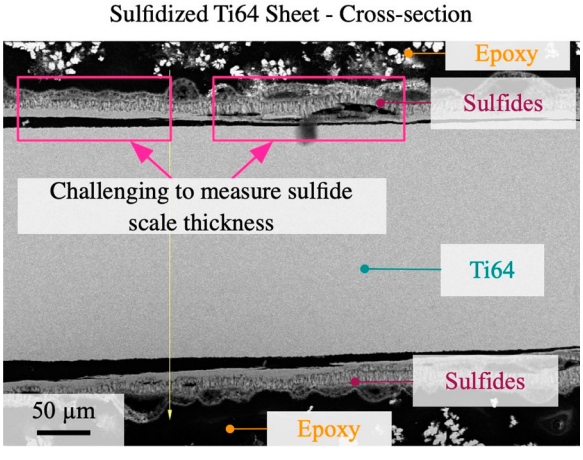

Figure 3. SEM backscattered electron image of the cross-section of sulfidized Ti64 sheet showing the fragility of the scale by its separation of the scale from the metal.

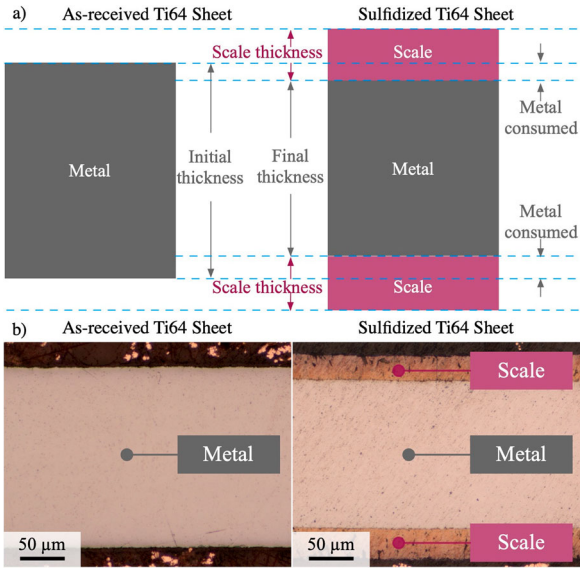

Figure 4. Schematic representation (a) and the optical image (b) of the material consumption approach showing the as-received and sulfidized metal.

diffusion coefficient.

$$C_{Ti} = \frac{Dc}{G}\left(\frac{M_{sulfide}\cdot\rho_{metal}}{n\cdot M_{metal}\cdot\rho_{sulfide}}\right)^2 \quad (7)$$

Substitution of Equation 5 into Equation 2 gives Equation 8 which predicts the metal consumed thickness for a given sulfidation time at one temperature since the consumption coefficient is a temperature-dependent quantity:

$$y^2_{metal} = 2C_{Ti}t \quad (8)$$

To predict the metal consumed thickness for a given sulfidation time and a given sulfidation temperature, the temperature dependence of the consumption coefficient is made explicit by using the Arrhenius law. Equation 9 gives the Arrhenius form of the consumption coefficient.

$$C_{Ti} = C_o e^{\left[\frac{-E_a}{RT}\right]} \quad (9)$$

where C_o = pre-exponential factor $[m^2\cdot s^{-1}]$, E_a = apparent activation energy $[J\cdot mol^{-1}]$, R = universal gas constant $[J\cdot K^{-1}\cdot mol^{-1}]$, and T = temperature $[K]$. Then, substituting Equation 9 in Equation 8, the metal consumption model was derived that predicted the metal consumption thickness for a given sulfidation temperature and sulfidation time:

$$y^2_{metal} = 2C_o e^{\left[\frac{-E_a}{RT}\right]}t \quad (10)$$

The apparent activation energy and the pre-exponential factor in the metal consumption model can be determined empirically. In Arrhenius law, the slope of the linearised equation gives the apparent activation energy, and the y-intercept gives the pre-exponential factor.

Results and discussion

The metal consumption measurement should be advantageous for the scale thickness measurement for determining kinetic parameters since the material consumption approach works regardless of the fragility of the scales. To validate the material consumption approach, the kinetics of a titanium-sulfur system were measured and compared to Ohta et al. [19] and Dutrizac's [20] work.

Validation of material consumption approach with titanium-sulfur system

A titanium-sulfur system was studied to verify the apparent activation energy estimated from the material consumption approach. Figure 5 shows the Arrhenius plot with $log_e C_{Ti}$ against 1/T on the x-axis for the titanium-sulfur system. The apparent activation energy estimated by the material consumption approach was 116.2 kJ·mol$^{-1,}$ and the pre-exponential factor estimated was 1.2×10^{-9} m^{2}s^{-1}. Dutrizac [20] estimated the apparent activation energy to be 112.9 and 138.1 kJ·mol^{-1} for annealed and unannealed titanium, respectively. Ohta et al. [19] estimated the apparent activation energy for the growth of the compact layer to be 100.4 kJ·mol^{-1} for unannealed titanium. These results are tabulated in Table 1 for clarity and ease of comparison. Both researchers studied the sulfidation of titanium with sulfur vapour by measuring the mass change of the sample. The apparent activation energy estimated from the material consumption approach closely matched that of Dutrizac [20] and Ohta et al. [19]. These results validate the material consumption approach.

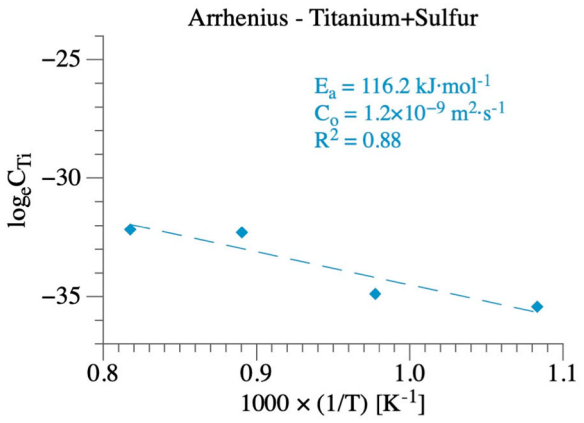

Figure 5. Plot of consumption model showing the apparent activation energy, $E_a = 116.2$ kJ·mol^{-1} and $C_o = 1.2\times10^{-9}$ m^{2}s^{-1} for the titanium-sulfur system.

Table 1. Activation energies of the titanium-sulfur system compared to literature.

Author	Activation energy, Ea[kJ·mol^{-1}]
This work	116.2
Dutrizac [20]	112.9
Dutrizac [20]	138.1
Ohta et al. [19]	100.4

Sulfidation kinetics of Ti-6Al-4V

The material consumption approach was used on the Ti64-sulfur system to estimate the apparent activation energy and the pre-exponential factor. Figure 6 shows the Arrhenius plot for the Ti64-sulfur system. The apparent activation energy estimated by the material consumption approach was 110.4 kJ·mol^{-1} and the pre-exponential factor estimated was 1.3×10^{-9} m^{2}s^{-1}. The apparent activation energy for the Ti64-sulfur system was lower than that of the titanium-sulfur system. The higher pre-exponential factor in the Ti64-sulfur system, which is analogous to collision frequency/jump frequency, is indicative of faster and higher material consumption in the Ti64-sulfur system than the titanium-sulfur system. The activation energies and pre-exponential factors

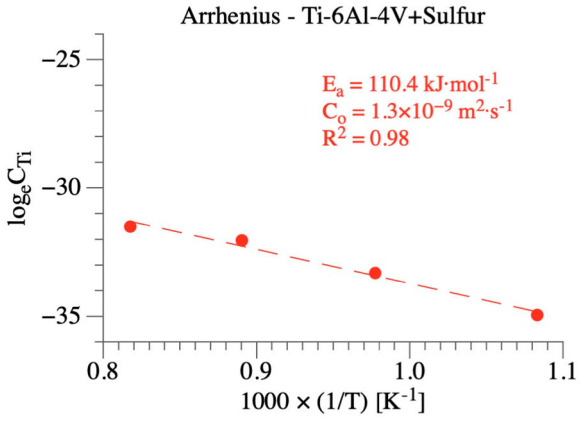

Figure 6. Plot of consumption model showing the apparent activation energy, $E_a = 116.2$ kJ·mol^{-1} and $C_o = 1.3\times10^{-9}$ m^{2}s^{-1} for the Ti64-sulfur system.

Table 2. Activation energies and pre-exponential factors of the titanium-sulfur and Ti64-sulfur systems.

System	Activation energy, Ea [kJ·mol^{-1}]	Pre-exponential factor, Co [m^2·s^{-1}]
Titanium-sulfur	110.4	1.3×10^{-9}
Ti64-sulfur	116.2	1.2×10^{-9}

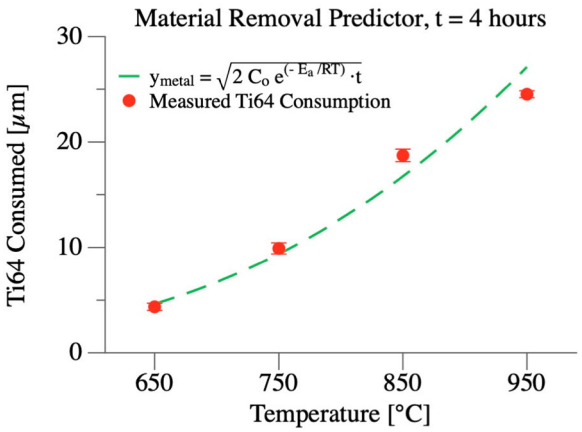

Figure 7. The experimentally measured Ti64 consumption for a 4-hour sulfidation closely matched the consumption from the empirical model based on the consumption model parameters (E_a and C_o).

for titanium-sulfur and Ti64-sulfur systems are tabulated in Table 2 for clarity and ease of comparison.

Material removal predictor

Using the kinetic parameters obtained from the material consumption approach for the Ti64-sulfur system (E_a and C_o) in the metal consumption model, a material removal predictor was developed that showed the amount of Ti64 consumed at different sulfidation temperatures for a sulfidation time of 4 h, as shown in Figure 7. The experimentally measured material removed closely matched the predicted material removed from the material consumption model. Thus, the material removal predictor, Equation 11, can help designers with oversizing a part and technicians with the necessary sulfidation temperature, time, and the number of cycles to remove a required amount of material from the surface of the Ti64 part.

$$y_{metal} = \sqrt{2C_o e^{\{\frac{-E_a}{RT}\}} t} \tag{11}$$

Conclusions

The apparent activation energy of sulfidation for titanium-sulfur and Ti64-sulfur systems were estimated using the change in metal consumed thickness instead of the more common approach involving mass change. This metal consumption approach removed the need to measure scale thicknesses and is useful in systems with fragile scales. The apparent activation energy of sulfidation and the pre-exponential factor were estimated to be 110.4 kJ·mol^{-1} and 1.3×10^{-9} m^{2}s^{-1} for the titanium-sulfur system, and 116.2 kJ·mol^{-1} and 1.2×10^{-9} m^{2}s^{-1} for the Ti64-sulfur system. A material removal predictor was developed to estimate the amount of material removed for a given sulfidation temperature and time that will help designers and engineers choose the process parameters.

Disclosure statement

No potential conflict of interest was reported by the author(s).

Funding

Hildreth group gratefully acknowledges the support from the Department of Energy under contract agreement Grant #: DE-EE0008166 and the Department of Energy's Kansas City National Security Campus, operated by Honeywell Federal Manufacturing & Technologies, LLC, under contract number DE-NA0002839. In addition, the Hildreth group gratefully acknowledges the financial support from the National Science Foundation (CAREER: 1944516).

ORCID

Owen J. Hildreth http://orcid.org/0000-0001-5358-9080

References

[1] Medvedovski E, Mendoza GL, Rzad E, et al. Influence of multilayered thermal diffusion coatings on high-temperature sulfidation resistance of steels. Surf Coat Technol. 2020;403:126430, doi:10.1016/j.surfcoat.2020.126430

[2] Gesmundo F, Young DJ, Roy SK. The high temperature corrosion of metals in sulfidizing-oxidizing environments: a critical review. High Temp Mater Proc. 1989;8:149–190. doi:10.1515/HTMP.1989.8.3.149

[3] Lefky CS, Zucker B, Wright D, et al. Dissolvable supports in powder bed fusion-printed stainless steel. 3D Print Addit Manuf. 2017;4:3–11. doi:10.1089/3dp.2016.0043

[4] Yazdanparast S, Raikar S, Heilig M, et al. Iodine-based sensitization of copper alloys to enable self-terminating etching for support removal and surface improvements of additively manufactured components. 3D Print Addit Manufact. 2022. doi:10.1089/3dp.2021.0242

[5] Raikar S, Heilig M, Mamidanna A, et al. Self-terminating etching process for automated support removal and surface finishing of additively manufactured Ti-6Al-4 V. Addit Manuf. 2021;37:101694, doi:10.1016/j.addma.2020.101694

[6] Raikar S, DiGregorio S, Agnani M, et al. Improving fatigue performance of additively manufactured Ti-6Al-4V using sulfur-based self-terminating etching processes. Addit Manuf. 2023;61:103331, doi:10.1016/j.addma.2022.103331

[7] Izumi T, Yoshioka T, Hayashi S, et al. Oxidation behavior of sulfidation processed TiAl–2 at.% X (X = V, Fe, Co, Cu, Nb, Mo, Ag and W) alloys at 1173 K in air. Intermetallics. 2001;9:547–558. doi:10.1016/s0966-9795(01)00023-1

[8] Izumi T, Yoshioka T, Hayashi S, et al. Sulfidation properties of TiAl–2 at.% X (X = V, Fe, Co, Cu, Nb, Mo. sulfidation properties of TiAl–2 at.% X (X = V, Fe, Co, Cu, Nb, Mo, Ag and W) alloys at 1173 K and 1.3 Pa sulfur pressure in an H2S–H2 gas mixture. Intermetallics. 2000;8:891–901. doi:10.1016/S0966-9795(00)00028-5

[9] Du HL, Datta PK, Lewis DB, et al. High-temperature corrosion of Ti and Ti-6Al-4V alloy. Oxid Met. 1996;45:507–527. doi:10.1007/bf01046849

[10] Falk F, Sobol O, Stephan-Scherb C. The impact of the microstructure of Fe-16Cr-0.2C on high-temperature oxidation – sulphidation in SO_2. Corros Sci. 2021;190:109618, doi:10.1016/j.corsci.2021.109618

[11] Guo XH, Ren YJ, Shen J, et al. The corrosion behavior of Co-Cr-Al alloys exposed to mixed oxygen-sulfur atmospheres at 900 °C. Corros Sci. 2021;188:109530, doi:10.1016/j.corsci.2021.109530

[12] Birks N, Meier GH, Pettit FS. Introduction to the high temperature oxidation of metals. Cambridge: Cambridge University Press; 2006.

[13] Rusiecki S, Wójtowicz A, Mrowec S, et al. New thermobalance for studying the kinetics of high temperature reactions in sulphur

atmospheres. Solid State Ion. 1986;21:273–277. doi:10.1016/0167-2738(86)90189-X
[14] Mrowec S. A. calculations of parabolic rate constants for metal oxidation. Oxid Met. 1974;8:379–391. doi:10.1007/BF00603388
[15] Romanski J. Geometrical factors in studies of the kinetics of oxidation of metals at high temperatures. Parts 1 and 2. Parts 8 and 2. Corros Sci. 1968;8:67–87. doi:10.1016/s0010-938x(68)80074-5
[16] Naumenko D, Gleeson B, Wessel E, et al. Correlation between the microstructure, growth mechanism, and growth kinetics of alumina scales on a FeCrAlY alloy. and growth kinetics of alumina scales on a FeCrAlY alloy. Metall Mater Trans. 2007;38:2974–2983. doi:10.1007/s11661-007-9342-z
[17] O'Hare R. Materials kinetics fundamentals. Hoboken, New Jersey: John Wiley & Sons; 2014.
[18] Cramer SD; Covino BS, editors. Corrosion: fundamentals, testing, and protection; Ohio: ASM International ; 2003; p. 115–116.
[19] Ohta K, Fueki K, Mukaibo T. Sulfurization of titanium in sulfur vapor. Denki Kagaku Oyobi Kogyo Butsuri Kagaku. 1973;41:697–701. doi:10.5796/kogyobutsurikagaku.41.697
[20] Dutrizac JE. The reaction of titanium with sulphur vapour. J Less Common Met. 1977;51:283–303. doi:10.1016/0022-5088(77)90090-X
[21] Gates-Rector S, Blanton T. The powder diffraction file: a quality materials characterization database. Powder Diffr. 2019;34:352–360. doi:10.1017/S0885715619000812
[22] Strafford KN. The sulphidation of metals and alloys. Metall Rev. 1969;14:153–174. doi:10.1179/mtlr.1969.14.1.153
[23] Pilling N, Bedworth RJ. The oxidation of metals at high temperature. J Inst Met. 1923;29:529–582.